

## Electronic Supplementary Information (ESI)

### **A new rigid diindenocarbazole donor moiety for high quantum efficiency thermally activated delayed fluorescence emitter**

Kwang Jeong Kim<sup>a</sup>, Gyeong Heon Kim<sup>b</sup>, Raju Lampande<sup>b</sup>, Dae Hyun Ahn<sup>b</sup>, Joon Beom Im<sup>b</sup>,  
Ji Su Moon<sup>b</sup>, Jae Kyun Lee<sup>c</sup>, Jae Yeol Lee<sup>\*a</sup>, Ju Young Lee<sup>\*b</sup>, and Jang Hyuk Kwon<sup>\*b</sup>

<sup>a</sup>Department of Chemistry, Kyung Hee University, Hoegi-dong, Dongdaemun-gu, Seoul, 02447, Republic of Korea. Email: lly@khu.ac.kr

<sup>b</sup>Department of Information Display, Kyung Hee University, 26, Kyungheedae-ro, Dongdaemoon-gu, Seoul, 02447, Republic of Korea.

E-mail: juyoung105@khu.ac.kr, jhkwon@khu.ac.kr

<sup>c</sup>Center for Neuro-Medicine, Brain Science Institute, Korea Institute of Science and Technology, 131, Cheongyang, Seoul 02792, Republic of Korea

## **Table of Contents**

### **1. Experimental section**

#### **1.1. Material characterization**

#### **1.2. Device fabrication and characterization**

#### **1.3. Computational analysis**

#### **1.4. Calculations of rate constants and quantum efficiency fractions**

#### **1.5. Crystal structure determination**

### **2. Material synthesis**

## **1. Experimental section**

### **1.1. Material characterization**

UV-vis absorption and photoluminescence (PL) spectra were measured using SCINCO S-4100 spectrometer and JASCO FP8500 spectrometer, respectively. The transient PL decay of 100 nm thick emitter doped into host film was measured using Quantaaurus-Tau fluorescence lifetime measurement system (C11367-03, Hamamatsu Photonics Co.) in N<sub>2</sub> filled condition. Electrochemical analyses of the synthesized TADF emitters were inspected using cyclic voltammetry (CV). CV measurements were performed using EC epsilon electrochemical analysis equipment. To measure the CV characteristics of TADF emitters, platinum, carbon wire and Ag wire in 0.01 M AgNO<sub>3</sub>, 0.1 M tetrabutyl ammonium perchlorate (Bu<sub>4</sub>NClO<sub>4</sub>), acetonitrile solution were used as counter, working and reference electrodes, respectively. For supporting electrolyte, 0.1 M tetrabutyl ammonium perchlorate in acetonitrile solution was used. Using an internal ferrocene/ferrocenium (Fc/Fc<sup>+</sup>) standard, the potential values were converted to the saturated calomel electrode (SCE) scale. The optical band-gap was determined from the edge of absorption spectra. The LUMO level of each material was calculated from both the optical energy band gap and HOMO level.

### **1.2. Device fabrication and characterization**

To fabricate TADF-OLEDs, Indium-Tin-Oxide (ITO) covered glass substrates were cleaned in an ultrasonic bath with acetone and isopropyl alcohol. After cleaning, nitrogen blew on the substrates to remove residual impurities followed by UV-ozone treatment for 10 minutes. All organic layers and metal cathode were deposited on pre-cleaned ITO substrates. The vacuum evaporation system was used under  $\sim 1 \times 10^{-7}$  Torr vacuum pressure. The deposition rate of organic layer was around 0.5 Å/s. Especially, the deposition rate of LiF and Al were maintained at 0.1 Å/s and 5 Å/s, respectively. After the deposition process, all devices were

encapsulated using cover glass and UV resin. The emission area was 2 x 2 mm<sup>2</sup>. The current density versus voltage (J-V) and luminance versus voltage (L-V) characteristics were measured with Keithley 2635A SMU and Konica Minolta CS-100A, respectively. Electroluminescence (EL) spectra and Commission Internationale de l'Eclairage (CIE) 1931 color coordinate were obtained using Konica Minolta CS-2000 spectroradiometer.

### 1.3. Computational analysis

To calculate the molecular orbitals, and the energy levels of TADF emitters, density functional theory (DFT/B3LYP) simulations were performed with the double numerical plus d-functions (DND) atomic orbital basis set. The molecular simulations were done with DMol3 module in Material studio 8.0 software package (Accelrys Inc., San Diego, California, United States).

### 1.4. Calculations of rate constants and quantum efficiency fractions

The following equations describe the relationship between rate constants ( $k_p$ ,  $k_d$ ,  $k_{ISC}$ ,  $k_{RISC}$ ,  $k_r^s$ ,  $k_{nr}^T$ ) and quantum efficiency fractions ( $\Phi_p$ ,  $\Phi_d$ ,  $\Phi_{ISC}$ ,  $\Phi_{RISC}$ ).  $\tau_p$ ,  $\tau_d$ ,  $\Phi_p$ ,  $\Phi_d$  are measured values using time resolved PL decay measurement and integral sphere. Note that the rate constant of non-radiative decay at S<sub>1</sub> state ( $k_{nr}^S$ ) is assumed to be close to 0.

Equations

$$k_p = 1/\tau_p \quad (1)$$

$$k_d = 1/\tau_d \quad (2)$$

$$k_{ISC} = (1 - \Phi_p)k_p \quad (3)$$

$$k_{RISC} = \frac{k_p k_d \Phi_d}{k_{ISC} \Phi_p} \quad (4)$$

$$k_{nr}^T = k_d - \Phi_p k_{RISC} \quad (5)$$

$$\Phi_{ISC} = 1 - \Phi_p \quad (6)$$

$$\Phi_{RISC} = \Phi_d \Phi_{ISC} \quad (7)$$

In equation (1), (2),  $\tau$  and  $k$  are reciprocal relations. Crossing rates between systems can be calculated in order of (3), (4) and (5) and crossing quantum efficiencies between systems also can be calculated in order of (6), and (7) where  $k_{ISC}$  is intersystem crossing rate,  $k_{RISC}$  is reverse intersystem crossing rate and  $k_{nr}^T$  is non-radiative decay rate from lowest triplet state.  $\Phi_{ISC}$  and  $\Phi_{RISC}$  refer to intersystem crossing efficiency and RISC efficiency, respectively.<sup>1,2</sup>

### 1.5. Crystal structure determination

Crystal structure measurements were made on a Rigaku R-AXIS RAPID diffractometer using graphite monochromated Mo-K $\alpha$  radiation. The data were collected at a temperature of 297 K to a maximum  $2\Theta$  value of 54.9 °. The structure was solved by direct methods<sup>3</sup> and expanded using Fourier techniques. The non-hydrogen atoms were refined anisotropically. Hydrogen atoms were refined using the riding model. Neutral atom scattering factors were taken from International Tables for Crystallography (IT), Vol. C, Table 6.1.1.4.<sup>4</sup> All calculations were performed using the Crystal Structure<sup>5</sup> crystallographic software package except for refinement, which was performed using SHELXL Version 2014/7.<sup>6</sup>

## 2. Material synthesis

All chemicals, reagents, and solvents were purchased from commercial sources and used as received without further purification, unless otherwise mentioned. All reactions were monitored by thin-layer chromatography with silica gel 60 F254 (Merck, 0.2 mm). Column chromatography was carried out on silica gel (200-300 mesh). <sup>1</sup>H and <sup>13</sup>C-NMR spectra were measured using Bruker Avance 400 and JEOL JNM-ECZR 500 MHz. Additionally, high-resolution mass spectra were performed using JEOL JMS-600W Gas Chromatography-Mass spectrometer

### 2.1. Synthesis of 5-phenyl-10,15-dihydro-5*H*-diindolo[3,2-*a*:3',2'-*c*]carbazole (**1**) and 5,10-diphenyl-10,15-dihydro-5*H*-diindolo[3,2-*a*:3',2'-*c*]carbazole (**2**)

To a solution of 10,15-dihydro-5*H*-diindolo[3,2-*a*:3',2'-*c*]carbazole (2.51 g, 7.27 mmol), iodobenzene (1.63 g, 7.99 mmol), and sodium *tert*-butoxide (2.10 g, 21.8 mmol) in 1,4-dioxane (40 mL) were added palladium(II) acetate (0.0540 g, 0.240 mmol) and tri-*tert*-butylphosphine (0.146 g, 0.720 mmol) under Argon. After stirring at 100 °C for 24 hr, the reaction mixture was cooled to room temperature and concentrated under reduced pressure. The residue was purified by flash column chromatography (dichloromethane : hexane = 1:5 to 1:1) and recrystallized from dichloromethane and hexane to give **1** (1.30 g, 42%) as a white solid and **2** (0.72 g, 19%) as a white solid.

**1**: <sup>1</sup>H-NMR (400 MHz, DMSO-*d*<sub>6</sub>) δ 11.98 (1H, s), 11.92 (1H, s), 8.78 (1H, d, *J* = 8.0 Hz), 8.74 (1H, d, *J* = 8.0 Hz), 7.78 (1H, d, *J* = 8.0 Hz), 7.73-7.67 (5H, m), 7.64 (1H, d, *J* = 8.0 Hz), 7.44 (2H, t, *J* = 8.0 Hz), 7.37 (2H, t, *J* = 8.0 Hz), 7.31 (1H, d, *J* = 8.0 Hz), 7.17 (1H, t, *J* = 8.0 Hz), 6.64 (1H, t, *J* = 8.0 Hz), 5.76 (1H, d, *J* = 8.0 Hz); <sup>13</sup>C-NMR (100 MHz, DMSO-*d*<sub>6</sub>) δ 140.4, 140.1, 139.0, 138.8, 136.2, 134.8, 133.4, 130.1, 128.7, 128.6, 123.1, 123.0, 122.7,

122.3, 121.9, 121.4, 121.3, 120.5, 120.1, 119.9, 119.2, 118.5, 111.2, 110.7, 109.9, 101.8, 101.5, 100.8.

**2:**  $^1\text{H-NMR}$  (400 MHz,  $\text{DMSO-}d_6$ )  $\delta$  12.01 (1H, s), 8.87 (1H, d,  $J = 8.0$  Hz), 7.77-7.67 (11H, m), 7.49 (1H, t,  $J = 8.0$  Hz), 7.44 (1H, d,  $J = 8.0$  Hz), 7.40 (1H, d,  $J = 8.0$  Hz), 7.22 (1H, t,  $J = 8.0$  Hz), 7.18 (1H, t,  $J = 8.0$  Hz), 7.12 (1H, d,  $J = 8.0$  Hz), 6.72 (1H, t,  $J = 8.0$  Hz), 6.66 (1H, t,  $J = 8.0$  Hz), 5.96 (1H, d,  $J = 8.0$  Hz), 5.75 (1H, d,  $J = 8.0$  Hz);  $^{13}\text{C-NMR}$  (100 MHz,  $\text{DMSO-}d_6$ )  $\delta$  170.3, 140.9, 140.6, 140.2, 140.0, 139.3, 137.3, 135.8, 134.6, 130.2, 128.9, 128.7, 128.5, 128.4, 123.7, 122.9, 122.5, 121.8, 121.7, 121.5, 121.3, 120.8, 120.2, 119.7, 118.7, 110.9, 110.2, 109.6, 103.0, 102.3, 101.9.

## **2.2. Synthesis of 5,10-bis{4-(4,6-diphenyl-1,3,5-triazin-2-yl)phenyl}-15-phenyl-10,15-dihydro-5H-diindolo[3,2- $\alpha$ :3',2'-c]carbazole (DTRZ-DI)**

To a solution of 5-phenyl-10,15-dihydro-5H-diindolo[3,2- $\alpha$ :3',2'-c]carbazole (**1**, 1.30 g, 3.07 mmol), 2-(4-bromophenyl)-4,6-diphenyl-1,3,5-triazine (2.62 g, 6.75 mmol), and sodium *tert*-butoxide (1.947 g, 20.3 mmol) in *o*-xylene (20 mL) were added tri-*tert*-butylphosphine (0.123 g, 0.608 mmol) and tris(dibenzylideneacetone)dipalladium(0)-chloroform adduct (0.210 g, 0.203 mmol). After stirring at 130 °C for 36 hr under Ar, the reaction mixture was cooled to room temperature and concentrated under reduced pressure. The residue was purified by flash column chromatography (toluene : hexane = 1:4 to 1:1) and recrystallized from toluene and hexane to give **DTRZ-DI** (2.18 g, 68%) as a yellow solid.

$^1\text{H-NMR}$  (500 MHz,  $\text{CDCl}_3$ )  $\delta$  9.08 (4H, d,  $J = 8.0$  Hz), 8.81 (8H, d,  $J = 8.0$  Hz), 7.88 (4H, d,  $J = 8.0$  Hz), 7.73-7.67 (2H, m), 7.67-7.65 (2H, m), 7.65-7.61 (4H, m), 7.61-7.57 (8H, m), 7.53 (2H, t,  $J = 7.2$  Hz), 7.56-7.50 (2H, m), 7.37-7.32 (2H, m), 7.29 (1H, dd,  $J = 8.0$  and 6.9 Hz), 7.24-7.13 (3H, m), 6.90-6.73 (3H, m), 6.43 (2H, d,  $J = 8.0$  Hz), 6.09 (d,  $J = 8.0$  Hz, 1H);  $^{13}\text{C-NMR}$  (126 MHz,  $\text{CDCl}_3$ )  $\delta$  171.9, 170.9, 144.7, 141.8, 141.5, 140.9, 137.7, 137.4, 137.3,

136.2, 135.7, 134.3, 132.8, 130.7, 130.1, 129.8, 129.1, 128.8, 128.7, 128.6, 128.5, 128.4, 126.5, 123.6, 123.5, 123.0, 122.9, 122.8, 122.7, 122.3, 120.7, 120.6, 120.3, 110.1, 110.0, 105.3, 105.1, 105.0; HRMS (FAB+) calcd for C<sub>72</sub>H<sub>45</sub>N<sub>9</sub> (M+H) 1036.3876, found: 1036.3870.

### 2.3. Synthesis of 5-{4-(4,6-diphenyl-1,3,5-triazin-2-yl)phenyl}-10,15-diphenyl-10,15-dihydro-5*H*-diindolo[3,2-*a*:3',2'-*c*]carbazole (TRZ-DI)

TRZ-DI was synthesized by the same route as for DTRZ-DI but using 5,10-diphenyl-10,15-dihydro-5*H*-diindolo[3,2-*a*:3',2'-*c*]carbazole (**2**) instead of 5-phenyl-10,15-dihydro-5*H*-diindolo[3,2-*a*:3',2'-*c*]carbazole (**1**). A greenish yellow solid (38%), <sup>1</sup>H-NMR (400 MHz, CDCl<sub>3</sub>) δ 9.07 (2H, d, *J* = 8.0 Hz), 8.82 (4H, d, *J* = 8.0 Hz), 7.87 (2H, d, *J* = 8.0 Hz), 7.70-7.57 (16H, m), 7.53 (2H, d, *J* = 8.0 Hz), 7.35 (1H, d, *J* = 8.0 Hz), 7.34 (1H, d, *J* = 8.0 Hz), 7.22 (1H, d, *J* = 8.0 Hz), 7.18 (1H, d, *J* = 8.0 Hz), 7.14 (1H, t, *J* = 8.0 Hz), 6.81 (2H, t, *J* = 8.0 Hz), 6.77 (1H, d, *J* = 8.0 Hz) 6.41 (1H, d, *J* = 8.0 Hz), 6.07 (2H, d, *J* = 8.0 Hz); <sup>13</sup>C-NMR (100 MHz, CDCl<sub>3</sub>) δ 171.8, 170.8, 144.6, 141.7, 141.6, 141.3, 140.8, 137.7, 137.5, 137.2, 136.1, 135.5, 132.6, 130.6, 130.0, 129.0, 128.9, 128.7, 128.4, 128.3, 123.3, 123.2, 123.0, 122.7, 122.6, 122.5, 123.3, 122.2, 120.4, 120.1, 120.0, 109.9, 109.9, 109.8, 104.8, 104.7, 104.5; HRMS (FAB+) calcd for C<sub>57</sub>H<sub>37</sub>N<sub>6</sub> (M+H) 805.3080, found: 805.3085.

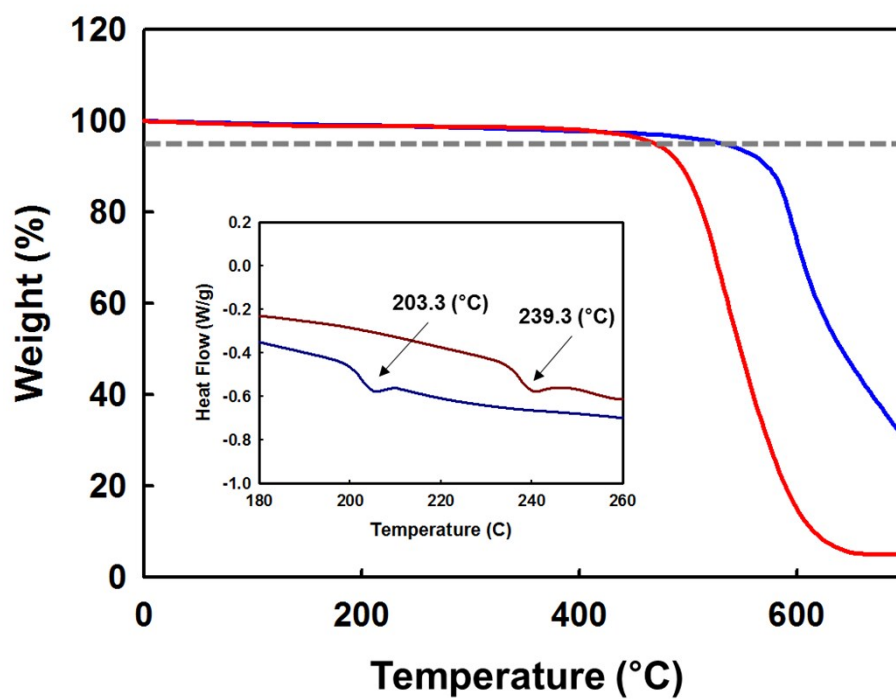


**Fig. S1.** DSC and TGA curves of DTRZ-DI (red line) and TRZ-DI (blue line).

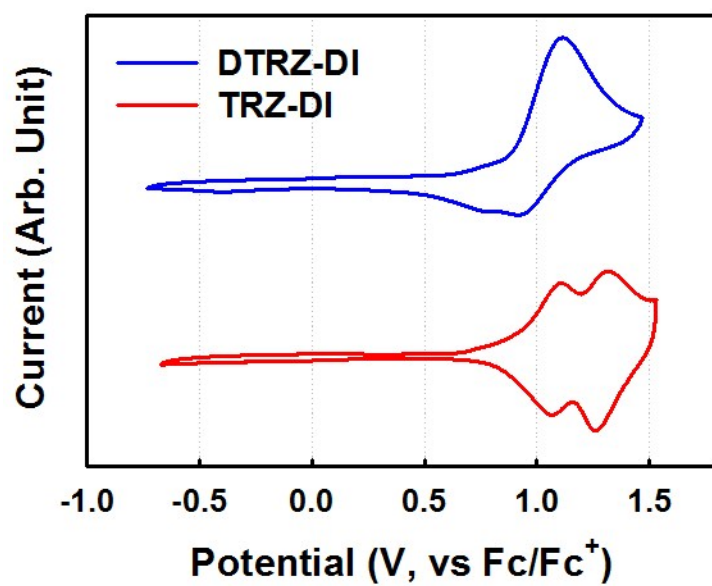


**Fig. S2.** Cyclic voltammetry analysis of DTRZ-DI and TRZ-DI.

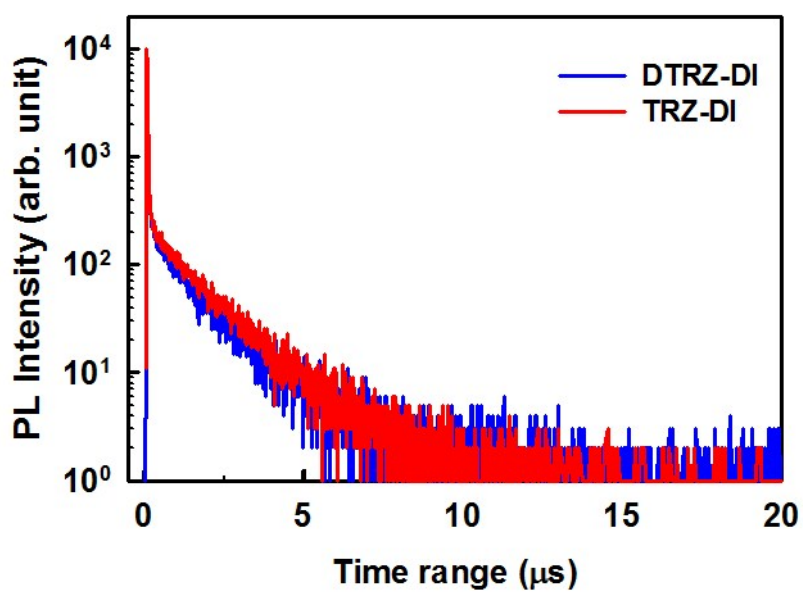


**Fig. S3.** Time-resolved PL decay curve of DTRZ-DI and TRZ-DI in toluene solution ( $1.0 \times 10^{-4}$  M) at room temperature.

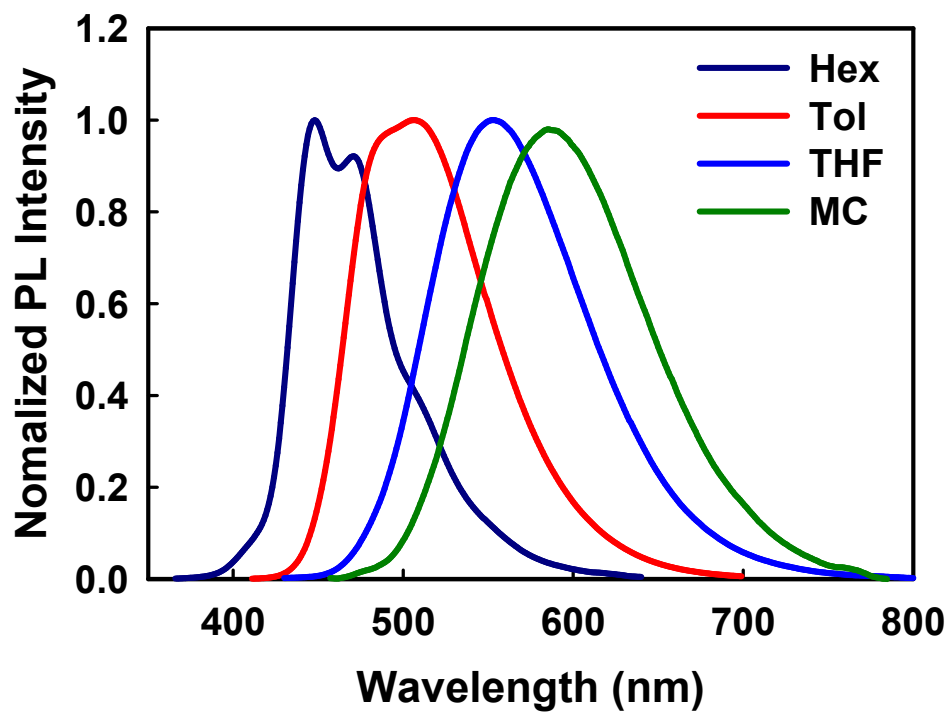


**Fig. S4.** PL spectrum of TRZ-DI emitter in different polarity solvents ( $1.0 \times 10^{-4}$  M).

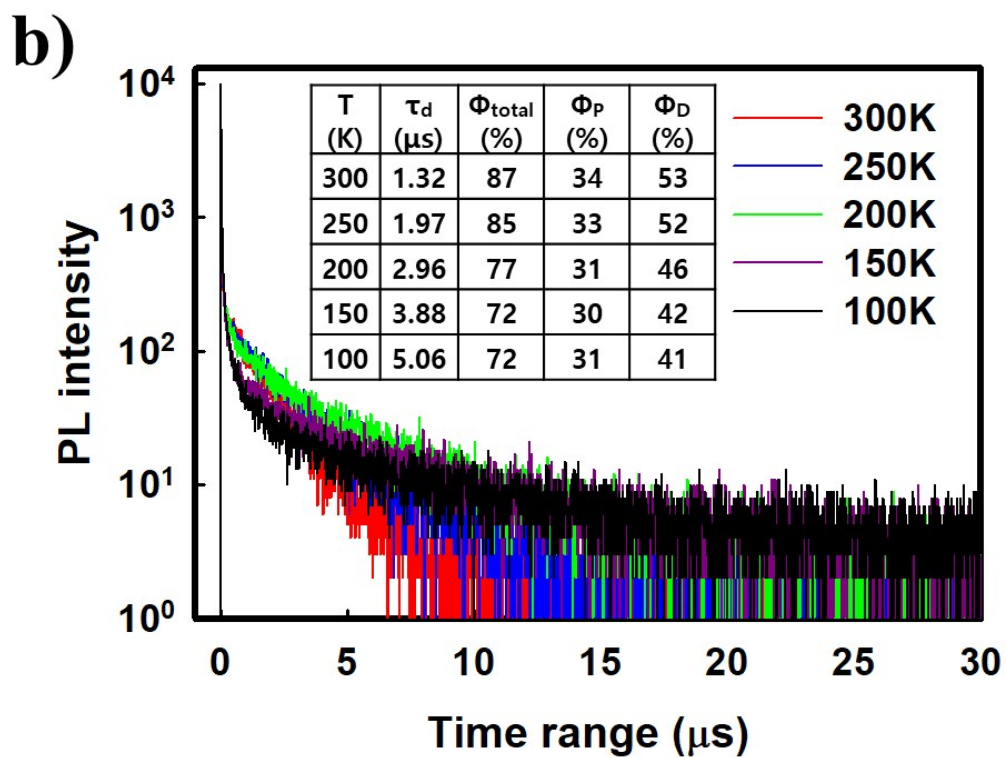
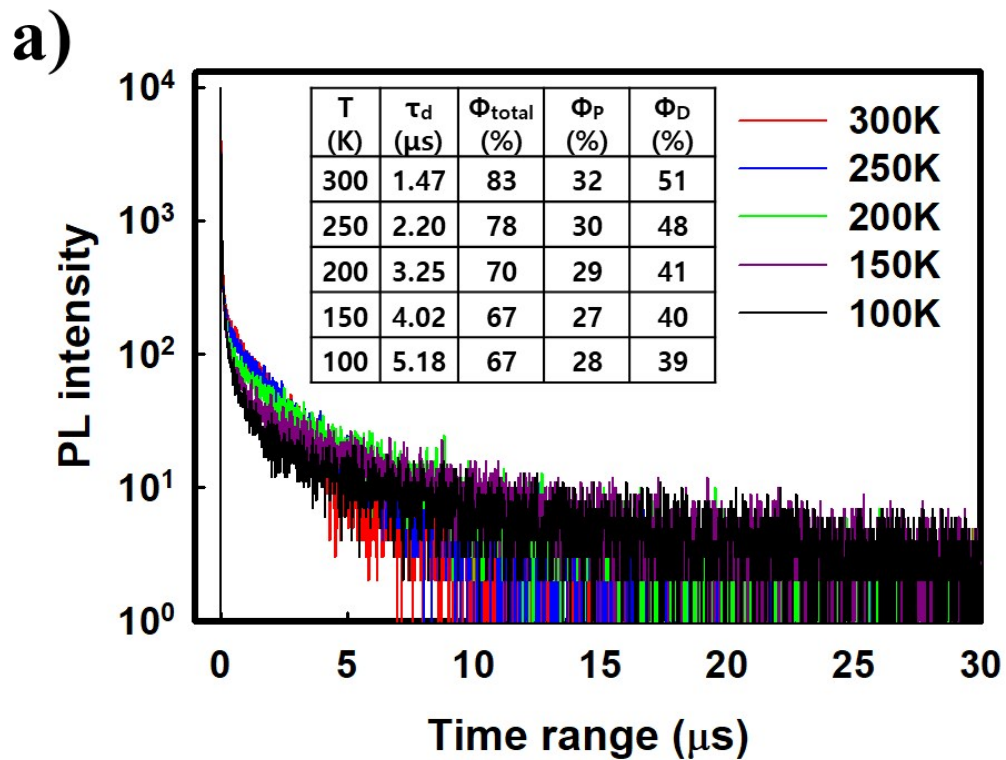


**Fig. S5.** Photoluminescence decay curves of emitter (25%) doped in TCTA:Bepp<sub>2</sub> film measured from 100 K to 300 K. (a) DTRZ-DI and (b) TRZ-DI. The inset table shows the delayed exciton lifetimes and PLQYs at different temperatures.

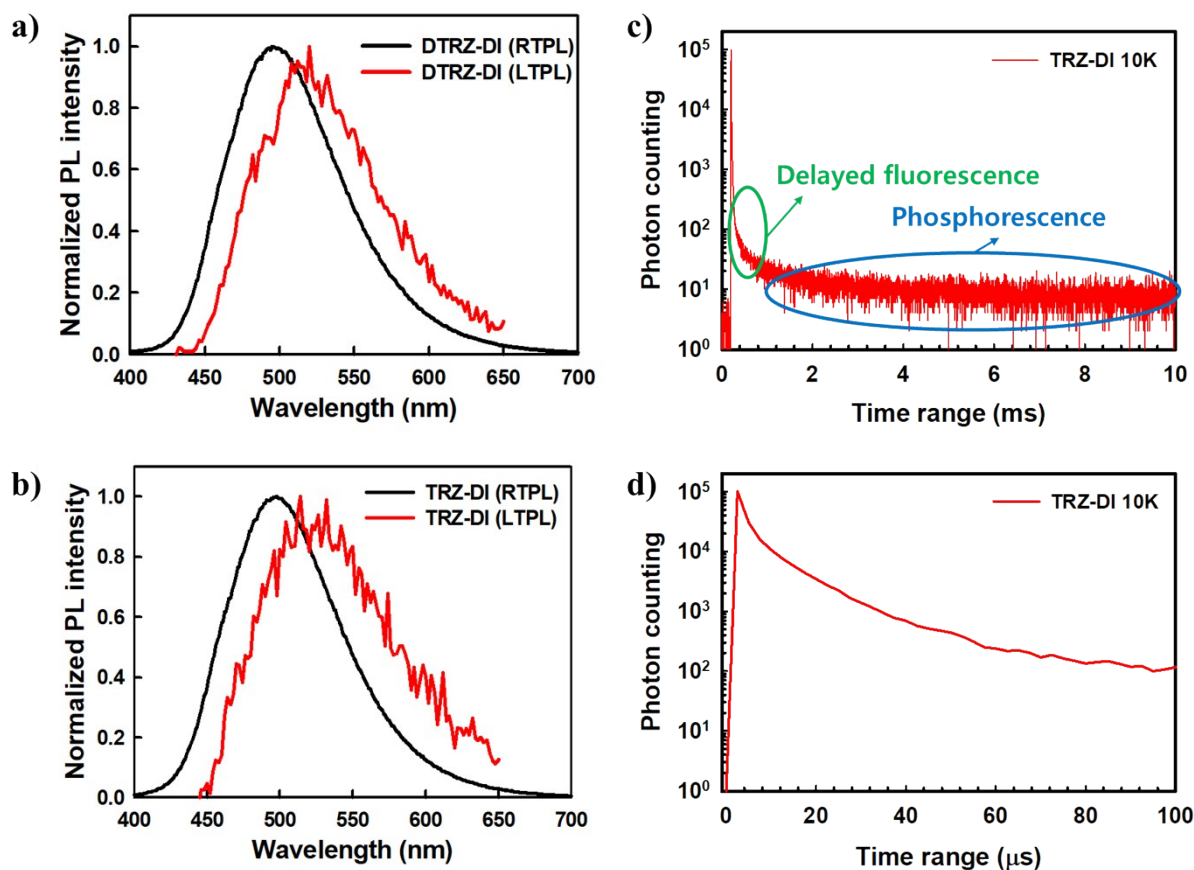


**Fig. S6.** Photoluminescence spectra of emitters in mCP: 6% doping films. (a) DTRZ-DI and b) TRZ-DI at room temperature (black line. 300 K) and low temperature (red line. 10 K). Phosphorescence emissions were obtained under 1 ms delayed condition. c) Phosphorescent emission decay ( $\sim 6.1$  ms lifetime) of TRZ-DI at 10K, d) Delayed fluorescent emission decay ( $\sim 15.3$   $\mu\text{s}$  lifetime) of TRZ-DI at 10K. This exciton decay lifetime of TRZ-DI was measured at 520 nm emission peak at 10 K.

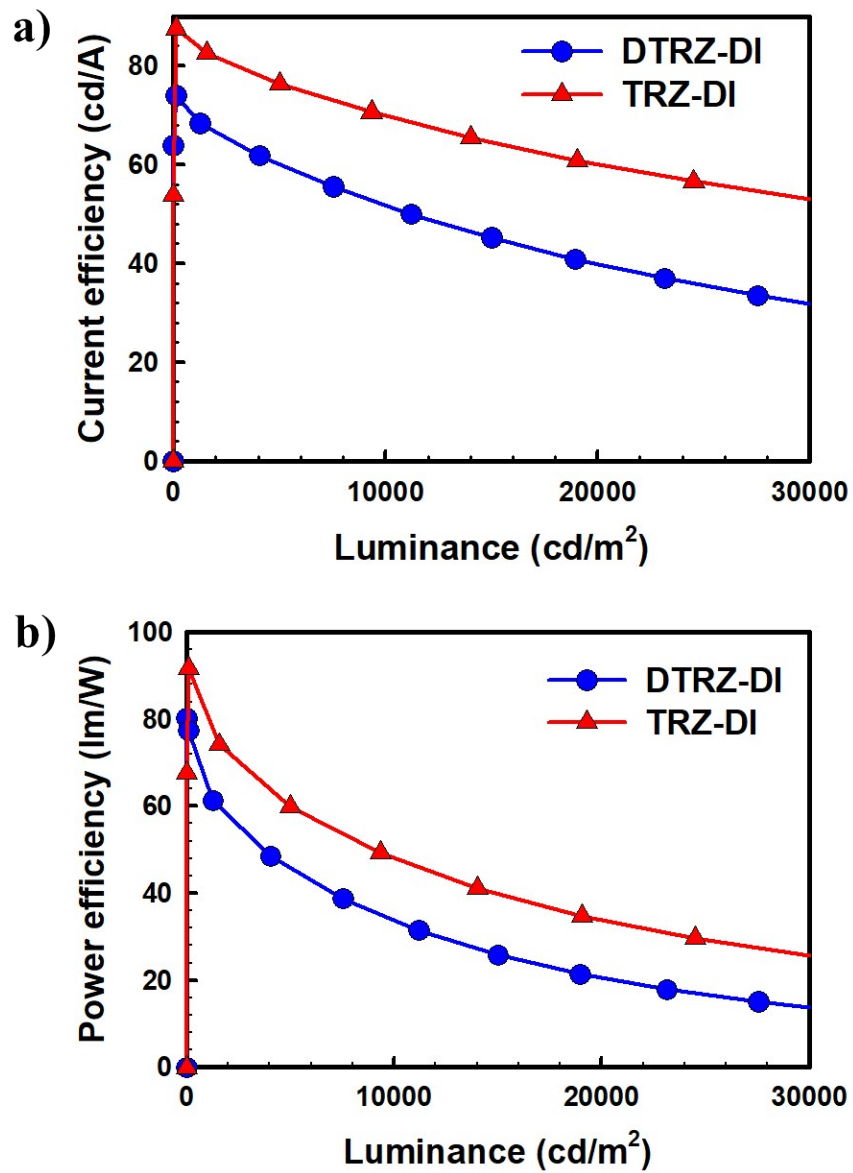


**Fig. S7.** (a) Current efficiency-luminance, b) Power efficiency-luminance characteristics of DTRZ-DI and TRZ-DI.

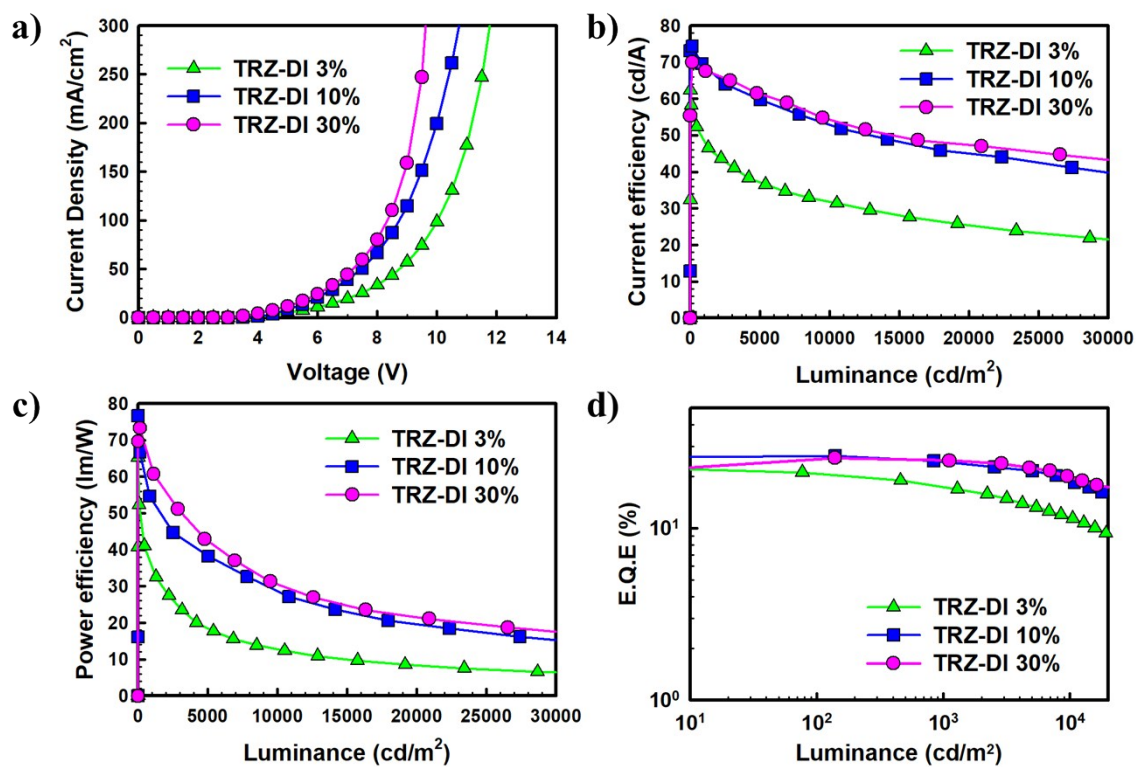


**Fig. S8.** Device performances of TADF-OLEDs with various doping concentration of emitters in TCTA: Bepp2 mixed host (3%, 10% and 30%) (a) Current density-voltage, (b) Current efficiency-luminance, (c) Power efficiency-luminance, (d) EQE-luminance characteristics.

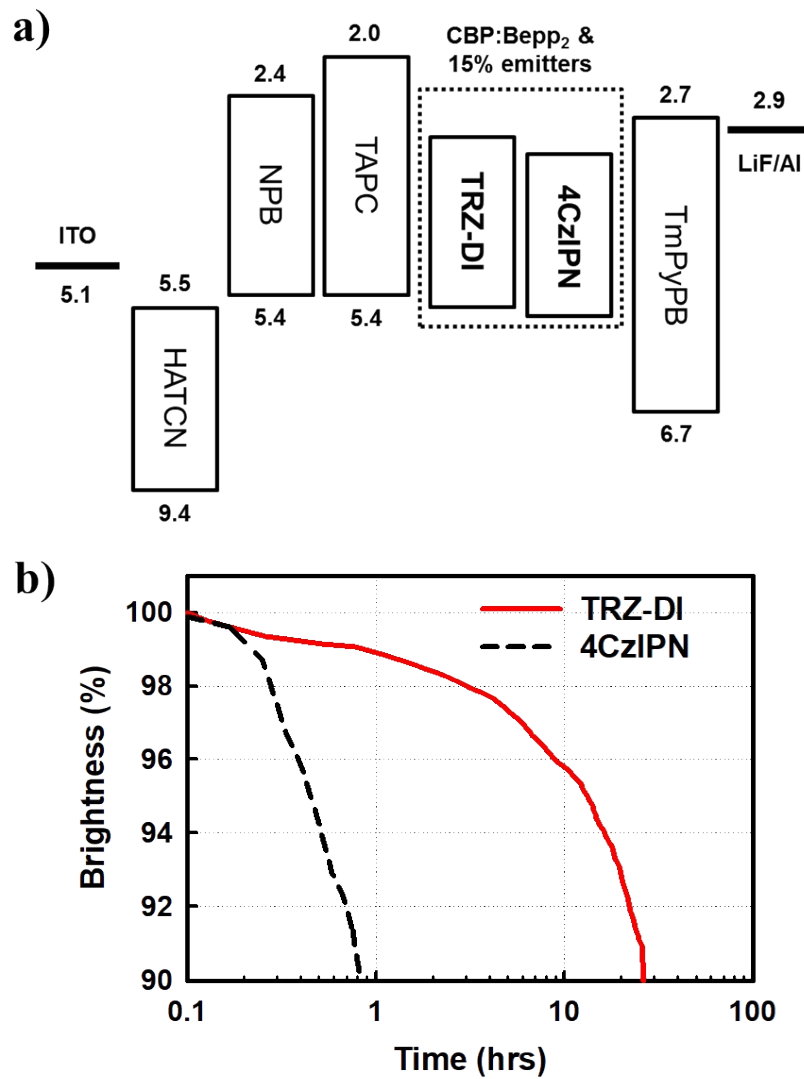


**Fig. S9.** (a) Device structure for the evaluation of operational lifetime (b) Operational lifetime result.

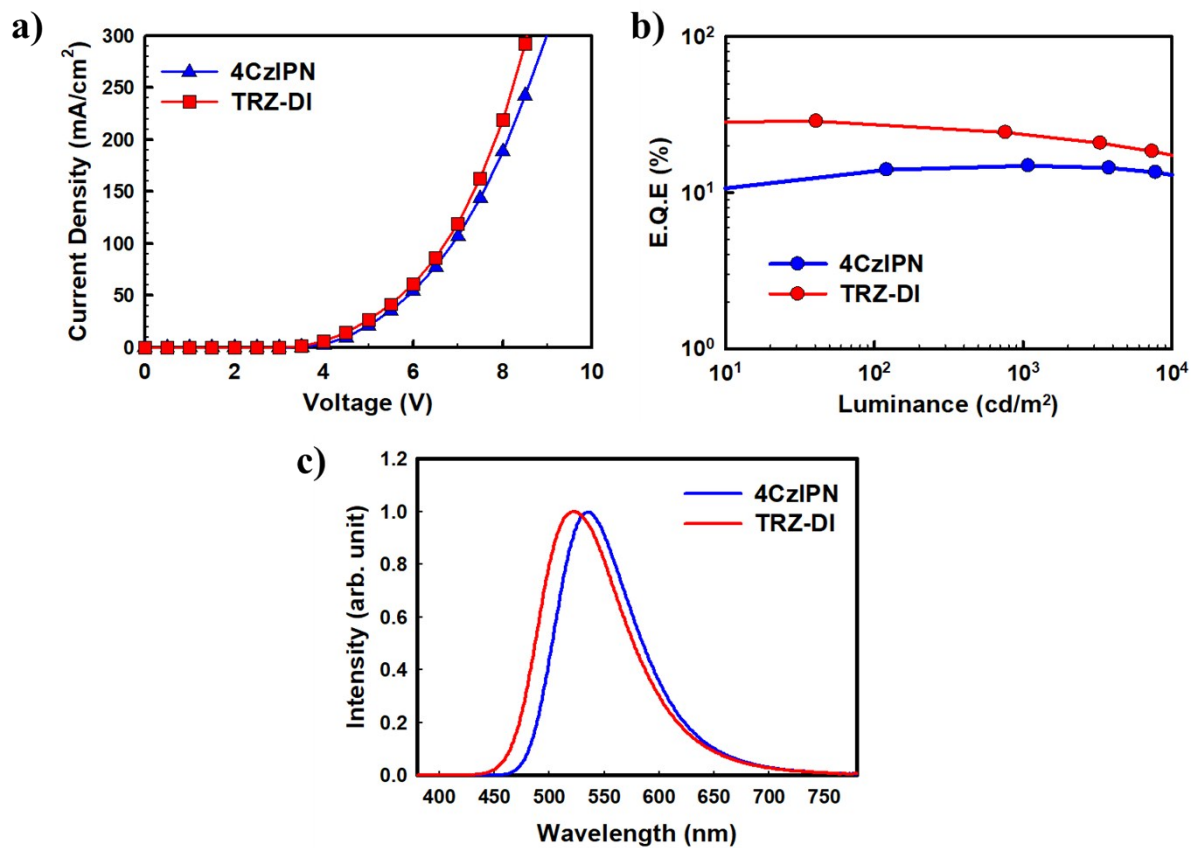


**Fig. S10.** The device performances of CBP:Bepp<sub>2</sub> based host system (a) Current density-voltage characteristics. (b) EQE-luminance characteristics. (c) EL spectrum.

**Table S1.** DFT calculation results of DTRZ-DI and TRZ-DI

| Emitters | HOMO<br>(eV) | LUMO<br>(eV) | $E_g$<br>(eV) | $T_1$<br>(eV) | $\Delta E_{ST}$<br>(eV) |
|----------|--------------|--------------|---------------|---------------|-------------------------|
| DTRZ-DI  | 4.80         | 1.87         | 2.93          | 2.85          | 0.08                    |
| TRZ-DI   | 4.78         | 1.83         | 2.95          | 2.89          | 0.06                    |

**Table S2.** Torsion angles ( $^{\circ}$ ) of TRZ-DI by single-crystal X-ray analysis.

|     |     |     |     |           |     |     |     |     |             |
|-----|-----|-----|-----|-----------|-----|-----|-----|-----|-------------|
| C5  | N1  | C6  | C7  | 175.5(2)  | C5  | N1  | C6  | C23 | -1.7(3)     |
| C6  | N1  | C5  | C4  | 177.7(2)  | C6  | N1  | C5  | C24 | -0.6(3)     |
| C5  | N1  | C40 | C39 | 110.6(2)  | C5  | N1  | C40 | C41 | -67.2(3)    |
| C40 | N1  | C5  | C4  | 23.0(4)   | C40 | N1  | C5  | C24 | -155.26(19) |
| C6  | N1  | C40 | C39 | -39.2(4)  | C6  | N1  | C40 | C41 | 143.0(2)    |
| C40 | N1  | C6  | C7  | -31.6(4)  | C40 | N1  | C6  | C23 | 151.2(2)    |
| C13 | N2  | C14 | C7  | -2.6(3)   | C13 | N2  | C14 | C15 | 175.6(2)    |
| C14 | N2  | C13 | C8  | -1.0(3)   | C14 | N2  | C13 | C12 | -179.6(2)   |
| C13 | N2  | C25 | C26 | -71.6(4)  | C13 | N2  | C25 | C30 | 107.8(3)    |
| C25 | N2  | C13 | C8  | -157.9(2) | C25 | N2  | C13 | C12 | 23.5(4)     |
| C14 | N2  | C25 | C26 | 135.4(3)  | C14 | N2  | C25 | C30 | -45.1(4)    |
| C25 | N2  | C14 | C7  | 153.4(2)  | C25 | N2  | C14 | C15 | -28.3(4)    |
| C21 | N3  | C22 | C15 | -3.4(3)   | C21 | N3  | C22 | C23 | 174.1(2)    |
| C22 | N3  | C21 | C16 | 0.8(3)    | C22 | N3  | C21 | C20 | -177.7(2)   |
| C21 | N3  | C31 | C32 | -72.2(3)  | C21 | N3  | C31 | C36 | 105.6(3)    |
| C31 | N3  | C21 | C16 | -148.4(2) | C31 | N3  | C21 | C20 | 33.1(4)     |
| C22 | N3  | C31 | C32 | 144.0(2)  | C22 | N3  | C31 | C36 | -38.2(3)    |
| C31 | N3  | C22 | C15 | 144.1(2)  | C31 | N3  | C22 | C23 | -38.4(4)    |
| C55 | N4  | C56 | N5  | -1.1(4)   | C55 | N4  | C56 | C43 | 178.2(2)    |
| C56 | N4  | C55 | N6  | 1.7(4)    | C56 | N4  | C55 | C37 | -177.8(2)   |
| C56 | N5  | C57 | N6  | 1.8(5)    | C56 | N5  | C57 | C49 | -178.6(2)   |
| C57 | N5  | C56 | N4  | -0.5(4)   | C57 | N5  | C56 | C43 | -179.8(2)   |
| C55 | N6  | C57 | N5  | -1.3(4)   | C55 | N6  | C57 | C49 | 179.1(2)    |
| C57 | N6  | C55 | N4  | -0.6(4)   | C57 | N6  | C55 | C37 | 178.9(2)    |
| C2  | C1  | C24 | C5  | -3.2(4)   | C2  | C1  | C24 | C23 | 177.3(3)    |
| C24 | C1  | C2  | C3  | -0.1(4)   | C1  | C2  | C3  | C4  | 2.3(5)      |
| C2  | C3  | C4  | C5  | -1.0(4)   | C3  | C4  | C5  | N1  | 179.5(3)    |
| C3  | C4  | C5  | C24 | -2.4(4)   | N1  | C5  | C24 | C1  | -177.1(2)   |
| N1  | C5  | C24 | C23 | 2.5(3)    | C4  | C5  | C24 | C1  | 4.5(4)      |
| C4  | C5  | C24 | C23 | -175.9(2) | C6  | C7  | C8  | C8  | -4.0(5)     |
| N1  | C6  | C7  | C14 | 178.6(2)  | N1  | C6  | C23 | C22 | -178.6(2)   |
| N1  | C6  | C23 | C24 | 3.3(3)    | C7  | C6  | C23 | C22 | 4.0(4)      |
| C7  | C6  | C23 | C24 | -174.2(2) | C6  | C7  | C8  | C8  | 172.9(3)    |
| C23 | C6  | C7  | C14 | -4.5(4)   | C6  | C7  | C8  | C9  | -6.4(6)     |
| C6  | C7  | C8  | C13 | 176.9(3)  | C6  | C7  | C14 | N2  | -176.8(2)   |
| C6  | C7  | C14 | C15 | 4.8(4)    | C8  | C7  | C14 | N2  | 5.1(3)      |
| C8  | C7  | C14 | C15 | -173.3(2) | C7  | C8  | C9  | C9  | 171.2(3)    |
| C14 | C7  | C8  | C13 | -5.5(3)   | C7  | C8  | C9  | C10 | 179.6(3)    |
| C7  | C8  | C13 | N2  | 4.0(3)    | C7  | C8  | C13 | C12 | -177.2(2)   |
| C9  | C8  | C13 | N2  | -173.4(2) | C8  | C13 | C12 | C12 | 5.3(4)      |
| C13 | C8  | C9  | C10 | -4.0(4)   | C8  | C9  | C10 | C11 | 0.6(5)      |
| C9  | C10 | C11 | C12 | 1.7(5)    | C10 | C11 | C12 | C13 | -0.5(5)     |
| C11 | C12 | C13 | N2  | 175.3(3)  | C11 | C12 | C13 | C8  | -3.1(5)     |
| N2  | C14 | C15 | C16 | -6.5(5)   | N2  | C14 | C15 | C22 | 177.4(2)    |
| C7  | C14 | C15 | C16 | 171.5(2)  | C7  | C14 | C15 | C22 | -4.6(4)     |
| C14 | C15 | C16 | C17 | -3.9(5)   | C14 | C15 | C16 | C21 | 179.7(3)    |
| C14 | C15 | C22 | N3  | -178.3(2) | C15 | C22 | C23 | C23 | 4.0(4)      |
| C16 | C15 | C22 | N3  | 4.5(3)    | C16 | C15 | C22 | C23 | -173.1(2)   |
| C22 | C15 | C16 | C17 | 172.5(3)  | C22 | C15 | C16 | C21 | -3.9(3)     |
| C15 | C16 | C17 | C18 | -178.1(3) | C16 | C21 | N3  | C21 | 1.9(3)      |

|     |     |     |     |             |     |     |     |     |           |            |
|-----|-----|-----|-----|-------------|-----|-----|-----|-----|-----------|------------|
| C15 | C16 | C21 | C20 | -179.5(2)   | C17 | C16 | C21 | N3  | -175.2(2) |            |
| C17 | C16 | C21 | C20 | 3.4(4)      |     | C21 | C16 | C17 | C18       | -2.1(4)    |
| C16 | C17 | C18 | C19 | -0.2(4)     |     | C17 | C18 | C19 | C20       | 1.3(5)     |
| C18 | C19 | C20 | C21 | -0.0(5)     |     | C19 | C20 | C21 | N3        | 176.0(3)   |
| C19 | C20 | C21 | C16 | -2.4(4)     |     | N3  | C22 | C23 | C6        | 179.1(2)   |
| N3  | C22 | C23 | C24 | -3.4(5)     |     | C15 | C22 | C23 | C6        | -3.7(4)    |
| C15 | C22 | C23 | C24 | 173.8(3)    |     | C6  | C23 | C24 | C1        | 176.0(3)   |
| C6  | C23 | C24 | C5  | -3.5(3)     |     | C22 | C23 | C24 | C1        | -1.7(6)    |
| C22 | C23 | C24 | C5  | 178.8(3)    |     | N2  | C25 | C26 | C27       | -179.7(2)  |
| N2  | C25 | C30 | C29 | 179.8(2)    |     | C26 | C25 | C30 | C29       | -0.7(4)    |
| C30 | C25 | C26 | C27 | 0.9(4)      |     | C25 | C26 | C27 | C28       | -0.7(5)    |
| C26 | C27 | C28 | C29 | 0.3(6)      |     | C27 | C28 | C29 | C30       | -0.1(6)    |
| C28 | C29 | C30 | C25 | 0.4(5)      |     | N3  | C31 | C32 | C33       | 177.21(18) |
| N3  | C31 | C36 | C35 | -178.45(18) |     | C32 | C31 | C36 | C35       | -0.6(3)    |
| C36 | C31 | C32 | C33 | -0.6(4)     |     | C31 | C32 | C33 | C34       | 1.3(4)     |
| C32 | C33 | C34 | C35 | -0.9(5)     |     | C33 | C34 | C35 | C36       | -0.4(5)    |
| C34 | C35 | C36 | C31 | 1.1(4)      |     | C38 | C37 | C42 | C41       | 0.4(4)     |
| C42 | C37 | C38 | C39 | -1.3(4)     |     | C38 | C37 | C55 | N4        | -169.3(3)  |
| C38 | C37 | C55 | N6  | 11.1(4)     |     | C55 | C37 | C38 | C39       | 178.3(2)   |
| C42 | C37 | C55 | N4  | 10.3(4)     |     | C42 | C37 | C55 | N6        | -169.3(3)  |
| C55 | C37 | C42 | C41 | -179.2(2)   | C37 | C38 | C39 | C40 | 0.6(4)    |            |
| C38 | C39 | C40 | N1  | -176.8(3)   | C38 | C39 | C40 | C41 | 1.0(4)    |            |
| N1  | C40 | C41 | C42 | 176.0(2)    | C37 | C39 | C40 | C41 | C42       | -1.8(4)    |
| C40 | C41 | C42 | C37 | 1.1(5)      |     | C44 | C43 | C48 | C47       | 0.9(5)     |
| C48 | C43 | C44 | C45 | -0.5(5)     |     | C44 | C43 | C56 | N4        | -3.2(4)    |
| C44 | C43 | C56 | N5  | 176.0(3)    |     | C56 | C43 | C44 | C45       | -179.5(3)  |
| C48 | C43 | C56 | N4  | 177.8(3)    |     | C48 | C43 | C56 | N5        | -2.9(5)    |
| C56 | C43 | C48 | C47 | 179.8(3)    |     | C43 | C44 | C45 | C46       | -0.5(5)    |
| C44 | C45 | C46 | C47 | 1.3(6)      |     | C45 | C46 | C47 | C48       | -1.0(6)    |
| C46 | C47 | C48 | C43 | -0.1(6)     |     | C50 | C49 | C54 | C53       | -1.0(5)    |
| C54 | C49 | C50 | C51 | 0.3(6)      |     | C50 | C49 | C57 | N5        | -1.5(5)    |
| C50 | C49 | C57 | N6  | 178.1(3)    |     | C57 | C49 | C50 | C51       | 177.3(3)   |
| C54 | C49 | C57 | N5  | 175.4(3)    |     | C54 | C49 | C57 | N6        | -5.0(5)    |
| C57 | C49 | C54 | C53 | -178.0(3)   | C49 | C50 | C51 | C52 | 0.3(7)    |            |
| C50 | C51 | C52 | C53 | -0.2(7)     |     | C51 | C52 | C53 | C54       | -0.6(6)    |
| C52 | C53 | C54 | C49 | 1.1(6)      |     |     |     |     |           |            |

**Table S3.** Device performances of TADF-OLEDs with various doping concentration of emitters in the mixed host.

| Emitters | Maximum efficiency     |                        |                      | Maximum Luminance [cd/m <sup>2</sup> ] | Roll-off ratio from Max. EQE |                            | CIE 1931 (x, y) <sup>d</sup> |
|----------|------------------------|------------------------|----------------------|--|------------------------------|----------------------------|------------------------------|
|          | CE <sup>a</sup> [cd/A] | PE <sup>b</sup> [lm/W] | EQE <sup>c</sup> [%] |  | @ 10,000 cd/m <sup>2</sup>   | @ 20,000 cd/m <sup>2</sup> |                              |
| 3%       | 62.3                   | 65.2                   | 22.5                 | 54,020                                 | 11.5                         | 9.2                        | (0.30, 0.54)                 |
| 10%      | 74.3                   | 76.6                   | 25.9                 | 77,070                                 | 19.0                         | 15.8                       | (0.32, 0.57)                 |
| 30%      | 70.0                   | 73.3                   | 25.6                 | 107,500                                | 19.9                         | 17.0                       | (0.33, 0.58)                 |

<sup>a</sup> Current efficiency; <sup>b</sup> Power efficiency; <sup>c</sup> External Quantum efficiency; <sup>d</sup> Measured at 10 mA/cm<sup>2</sup>.

**Table S4.** Thermal properties of TADF emitters.

| Emitters | T <sub>d</sub> <sup>a)</sup> [ °C ] | T <sub>g</sub> <sup>b)</sup> [ °C ] |
|----------|-------------------------------------|-------------------------------------|
| DTRZ-DI  | 528.3                               | 239.3                               |
| TRZ-DI   | 462.2                               | 203.0                               |

<sup>a)</sup>Decomposition temperature measured by TGA (thermogravimetric analysis) at 5% weight loss; <sup>b)</sup>Glass transition temperature scanned from DSC (differential scanning calorimetry).

**Table S5.** Electroluminescence properties of the green OLEDs with new emitters.

| Emitters | Maximum efficiency     |                        |                      | Maximum Luminance [cd/m <sup>2</sup> ] | Roll-off ratio from Max. EQE |                            | CIE 1931 (x, y) <sup>d</sup> |
|----------|------------------------|------------------------|----------------------|--|------------------------------|----------------------------|------------------------------|
|          | CE <sup>a</sup> [cd/A] | PE <sup>b</sup> [lm/W] | EQE <sup>c</sup> [%] |  | @ 10,000 cd/m <sup>2</sup>   | @ 20,000 cd/m <sup>2</sup> |                              |
| DTRZ-DI  | 73.9                   | 80.2                   | 26.2                 | 53,490                                 | 0.26                         | 0.46                       | (0.32, 0.58)                 |
| TRZ-DI   | 87.5                   | 91.6                   | 31.4                 | 71,160                                 | 0.19                         | 0.31                       | (0.31, 0.57)                 |

<sup>a</sup> Current efficiency; <sup>b</sup> Power efficiency; <sup>c</sup> External Quantum efficiency; <sup>d</sup> Measured at 10 mA/cm<sup>2</sup>.

**Table S6.** Device performances of TADF-OLEDs for the evaluation of operational lifetime.

| Emitters | Operating Voltage                               | External quantum efficiency      | CIE 1931 (x, y) <sup>a</sup> | Emission peak <sup>a)</sup> |
|----------|---|----------------------------------|------------------------------|-----------------------------|
|          | @ 1 cd/m <sup>2</sup> / 1,000 cd/m <sup>2</sup> | Max. / @ 1,000 cd/m <sup>2</sup> |                              |                             |
| TRZ-DI   | 2.6 / 3.6 V                                     | 28.7 / 24.1%                     | (0.31, 0.57)                 | 523 nm                      |
| 4CzIPN   | 2.9 / 4.0 V                                     | 14.8 / 14.7%                     | (0.35, 0.59)                 | 535 nm                      |

<sup>a)</sup>at 1,000 cd/m<sup>2</sup>.

## Reference

1. Q. Zhang, B. Li, S. Huang, H. Nomura, H. Tanaka, C. Adachi, *Nat. Photon.* 2014, **8**, 326.
2. K. Masui, H. Nakanotani, C. Adachi, *Org. Electron.* 2013, **14**, 2721.
3. G. M. Sheldrick, SHELXT Version 2014/4; *Acta Cryst.* 2014, **A70**, C1437.
4. A. J. C. Wilson, *International Tables for Crystallography*, Vol. C. Ed. Kluwer Academic Publishers, Dordrecht, A. Netherlands, 1992, pp. 572.
5. *Crystal Structure 4.2.3: Crystal Structure Analysis Package*, Rigaku Corporation (2000-2016). Tokyo 196-8666, Japan.
6. G. M. Sheldrick, SHELXL Version 2014/7, *Acta Cryst.* 2008, **A64**, 112.

